Automatic Detection for Ship Targets in RADARSAT SAR Images from Coastal Regions

Qingshan Jiang, Shengrui Wang, Djemel Ziou, and Ali El Zaart

Department of Mathematics and Computer Sciences
University of Sherbrooke
Sherbrooke, P.Q., J1K 2R1, Canada

Email: {*jiang, wang, ziou, elzaart*}@dmi.usherb.ca

Abstract

An automatic detection model for ship target in RADARSAT SAR images is described and assessed. The major tasks to be performed by this model are firstly to mask out land regions in a coastal image and secondly to detect ship targets in sea region. This paper presents current progress made on the detection model. Some detection examples of RADARSAT SAR images are also shown.

Keywords: SAR image, Cleaning operation, Land and sea detection, Ship target detection

1 Introduction

Ship detection is the detection of point targets in a radar clutter background. In general, ships are identified in the SAR imagery as very bright features because of the corner reflection. The detection of a ship depends on the physical properties of the ship itself such as size, shape, and structure, on the orientation relative to the radar look-direction, and also on the general sea state. There have already been considerable works done on the detection of ships and ship wakes in SAR images. For Seasat and ERS imagery, most of the research work is concentrated on the detection of ship wakes, e.g., [3, 6, 7, 8, 9], since they believe that it is advantageous to detect the wake instead of the ship since wake is larger and more distinct than the ship. RADARSAT has the capability to detect both stationary and moving ships on the ocean. These ships appear as bright targets, usually against the dark background of the ocean. However, The imaging geometry and polarization of RADARSAT makes wake detection more difficult than for the Seasat and ERS series of satellites.

Automatic detection algorithms for ships in RADARSAT SAR images have being developed by using statistical analysis and image processing techniques (see [1, 4, 5, 11]). This work is a further development of our research work in [1]. Our strategy is to detect all possible ship targets in RADARSAT SAR images (with 16 bits) from coastal regions (see Figure 1). The first problem in this automatic ship detection model is to distinguish sea from land in an image. One potential technique is presented in Section 3. The CFAR algorithms based on statistical models (K-distribution and Gamma distribution) are used to improve the ship detection performance. A ship detection algorithm is described in Section 4. Some experimental results based on our model are shown in Section 5.

Figure 1: A RADARSAT SAR image with land, sea and ship targets

2 Detection Algorithm

The model is composed of two principal processes: *land and sea detection* and *ship targets detection*. The structure of the current algorithm is illustrated in Figure 2. Different procedures are discussed accordingly in subsequent sections.

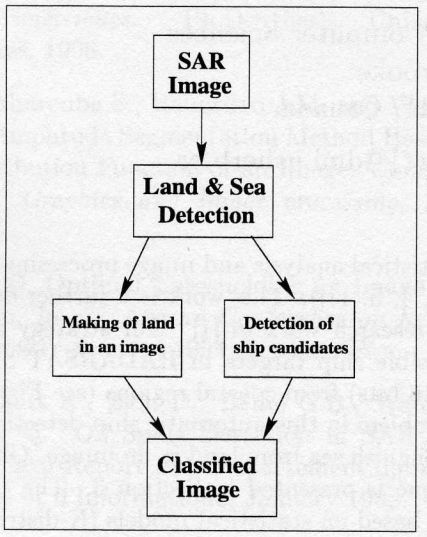

Figure 2: Block diagram of the ship detection system

3 Land and Sea Detection

The detection stars with the identification of land. It is obvious that the intensity values of these pixels in the land regions are higher than those in sea region. We first use a simple thresholding technique to select all possible pixels of land region. A thresholded image is defined as

$$g(x,y) = \begin{cases} L_1 & \text{if } f(x,y) \geq T \\ L_2 & \text{if } f(x,y) < T \end{cases}$$

where $f(x,y)$ is the intensity of the image at point (x,y), L_1 and L_2 are convenient intensity values and T corresponds to the threshold value. Objects inside the image are separated in two dominant groups based on the threshold setting, T. We take that $A = \{(x,y) \mid g(x,y) = L_1\}$ as the possible land region and $B = \{(x,y) \mid g(x,y) = L_2\}$ as the sea region, respectively. As discussed, ships are very bright features in SAR images so that pixels of possible ships may belong to A. On the other hand, the area of each possible ship target would be small. Therefore, we need to distinguish those small targets from the possible land region and put their pixels into sea region, B. For this purpose, a cleaning operation is applied to eliminate those false 'land' pixels. The cleaning operation is a logical filter which pertains to the structure and shape of objects (see [6]).

In our algorithm, we take the threshold value T as a medium between maximum and minimum of the intensity values of the image, and take $L_1 = 255 - T_0$ ($T_0 = T$ if $T \leq 255$, otherwise $T_0 = \frac{T}{256}$) and $L_2 = 255$. Meanwhile, the cleaning operation here is a 19 by 19 moving window. Each 'land' pixel in A is examined by placing it in the filter center. The filter then examines the 360 neighboring pixels. If more than 47 neighboring pixels are possible 'land' pixels, the center pixel is considered as a true land pixel. Otherwise, we put this pixel into the sea region B. Further, a morphological

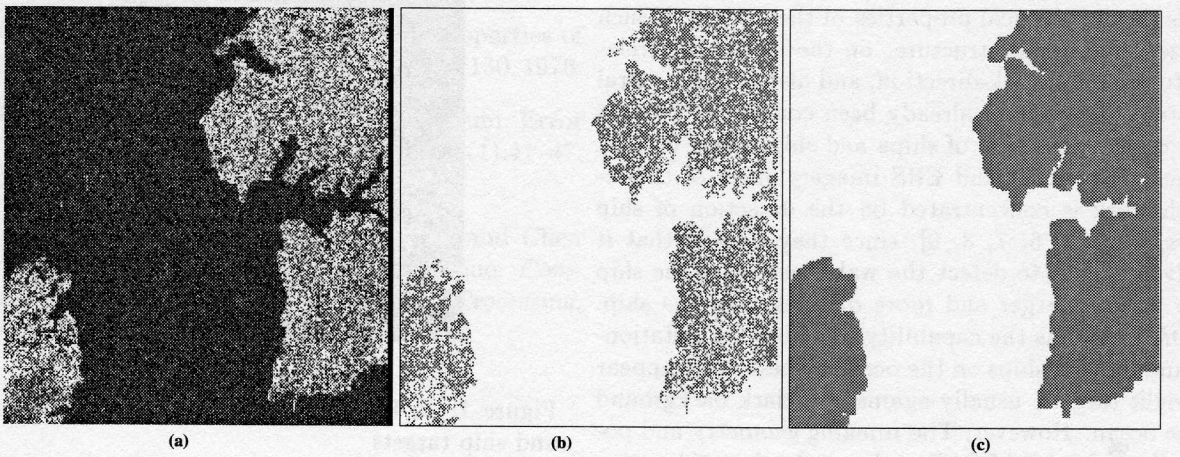

Figure 3: (a) Original image (1000 × 1000 pixels), (b) result by simple thresholding and cleaning, (c) final result of the land and sea detection

filter is applied to extend the land region. The filter is a 5 by 5 moving window. Each 'land' pixel is examined by placing it in the filter center. The filter then examines the 24 neighboring pixels. If more than 5 neighboring pixels are possible 'land' pixels, then all the pixels in this window are considered as 'land' pixels. The algorithm used for land and sea detection is described in detail in [12]. An example is shown in Figure 3.

4 Ship Target Detection

In general, ships are identified in the SAR imagery as very bright features because of the corner reflection. In reality, with an appropriate choice of threshold, all visible ships to human eye can be detected. A statistical algorithm for quantifying RADARSAT SAR's ship detection is proposed by Rey *et al* (see [4]). The initial ship detection algorithm (see [5]) in the *Ocean Monitoring Workstation* (OMW) is Constant False Alarm Rate (CFAR) algorithm based on K-distribution statistical fits, which is developed jointly by the *Defence Research Establishment Ottawa* (DREO) and the *Canada Centre for Remote Sensing* (CCRS).

In this section, we will identify all possible ship targets in the sea region as shown above. The CFAR technique has been used to improve ship target detection performance (see [1, 4, 5, 11]). This technique is used for the setting of thresholds, so that a radar operating in a sea-clutter environment will perform at a CFAR. Let $p(x)$ be a probability density function (pdf) for modeling ocean radar images, and let $F(x) = \int_0^x p(t)dt$. Then, $F(x)$ is an increasing continuous function on $[0, +\infty)$. Let η_c ($\eta_c \leq 1$) represent the required significance level. This significance level corresponds to a CFAR of $(1-\eta_c)$ for the pdf of intensity. We determine a threshold I_c by the solution to

$$\eta_c = \int_0^{I_c} p(x)dx. \quad (1)$$

For any given η_c, an approximate solution of I_c can be obtained by using dichotomy with the following step (see [11]):

Step 0: Find a positive integer I ($0 \leq I < 2^{16}$) such that

$$F(I) \leq \eta_c$$

and

$$F(I+1) > \eta_c.$$

Then, we take that I as the threshold I_c.

The main problems for CFAR technique are how to find a *pdf* with a goodness-of-fit for the histograms of SAR images and how to obtain a complete analysis solution for $F(x)$. We will first consider to use the K-distribution to test on data of the multi-look RADARSAT SAR ocean clutter returns. However, the modified Bessel function in this distribution often influences the computational speed or results in the computational overflow. Therefore, we will use the Gamma distribution to replace K-distribution when these estimated parameters (such as, μ, L, and ν) bring effect into the computation. More details on these statistical models are investigated in [12]. An introduction of these distributions is given in the following.

4.1 K-model

The compound K-distribution model (K-model) is an empirical model for sea clutter. It is applicable to high resolution radars that are capable of resolving fine structure on the sea surface. The *pdf* is a multi-look intensity K-distribution of the form (Rey *et al.*, 1996): for $x > 0$,

$$p(x) = \frac{2}{x\Gamma(\nu)\Gamma(L)}\left(\frac{L\nu x}{\mu}\right)^{\frac{L+\nu}{2}} K_{L-\nu}\left(2\sqrt{\frac{L\nu x}{\mu}}\right) \quad (2)$$

where μ is the image intensity mean, ν is a shape parameter, L is the number of statistically independent looks, $\Gamma(.)$ is the gamma-function, and $K_{\nu-L}(.)$ is the modified Bessel function. Its cumulative distribution does not have, in general, a closed form, since it is given by

$$\begin{aligned} F(x) &= C\int_0^t y^{\lambda}K_{\alpha}(y)dy \\ &= \frac{\lambda+\alpha-1}{(\lambda-\alpha+1)(\lambda+\alpha-1)}t^{\lambda+1}K_{\alpha}(t) \\ &\quad {}_1F_2\left(1; \frac{\lambda-\alpha+3}{2}, \frac{\lambda+\alpha+1}{2}; \frac{t^2}{4}\right) + \\ &\quad + \frac{1}{(\lambda-\alpha+1)(\lambda+\alpha+1)}t^{\lambda+2}K_{\alpha-1}(t) \\ &\quad {}_1F_2\left(1; \frac{\lambda-\alpha+3}{2}, \frac{\lambda+\alpha+3}{2}; \frac{t^2}{4}\right) \end{aligned}$$

where

- $t = 2\sqrt{\frac{L\nu x}{\mu}}$,
- $C = \frac{4}{2^{L+\nu}}\frac{1}{\Gamma(\nu)\Gamma(L)}$,
- $\alpha = \nu - L$,
- $\lambda = \nu + L - 1$;

and the hyper-geometric function is defined as

$${}_1F_2(a; b, c; z) = \sum_{k=0}^{+\infty}\frac{\Gamma(b)\Gamma(c)\Gamma(a+k)}{\Gamma(a)\Gamma(b+k)\Gamma(c+k)}\frac{z^k}{k!}.$$

The theoretical expressions for mean and variance of such *pdf* as shown in the equation (2) are as follows:

$$E[x] = \mu$$

and

$$Var[x] = \left[\left(1+\frac{1}{\nu}\right)\left(1+\frac{1}{L}\right)-1\right]\mu^2 \quad (3)$$

where E is the expectation and Var the variance operator. In our model, for a given data sample sequence $\{x_i\}_{i=0}^{M-1}$, we propose to estimate the look number L by

$$\hat{L} = \left\lceil \frac{\left(\frac{1}{M}\sum_{i=0}^{M-1} x_i\right)^2}{\frac{1}{M-1}\sum_{i=0}^{M-1}\left(x_i - \frac{1}{M}\sum_{i=0}^{M-1} x_i\right)^2} \right\rceil$$

based on $\nu > 0$ and the equation (3) (see [1]). Meanwhile, the parameter estimates of the mean and shape parameter can be obtained from the equations:

$$\hat{\mu} = \frac{1}{M}\sum_{i=0}^{M-1} x_i$$

and

$$\left(1+\frac{1}{\hat{\nu}}\right)\left(1+\frac{1}{\hat{L}}\right) = \frac{\frac{1}{M}\sum_{i=0}^{M-1} x_i^2}{\left(\frac{1}{M}\sum_{i=0}^{M-1} x_i\right)^2}.$$

4.2 Gamma-model

The probability density function (*pdf*) for the intensity in a 1-look SAR image is known to be an exponential distribution. For a multi-look intensity image, several distributions (Weibull, Gamma, Root of Gamma, K-distribution) are used to fit the SAR data, and statistical tests are conducted to determine those distributions that best fit the data. In this work, we first consider to use the K-distribution to fit the data. If those estimated parameters (μ, L, and ν) are large enough (e.g., *based on our experimental results, when the value of μ is larger than* 1000 *or the absolute value of* $(\nu - L)$ *is larger than* 200), we use the Gamma distribution to replace K-distribution.

The pdf is a multi-look intensity Gamma distribution of the form (Yanasse *et al.*, 1993): for $x > 0$,

$$f(x) = \frac{\beta^L}{\Gamma(L)} x^{L-1} exp(-\beta x) \quad (4)$$

where L is the number of statistically independent looks. Its cumulative distribution does not have, in general, a closed form, since it is given by

$$\begin{aligned} F(x) &= \int_0^x \frac{\beta^L}{\Gamma(L)} y^{L-1} exp(-\beta y) dy \\ &= \frac{1}{\Gamma(L)} \int_0^{\beta x} s^{L-1} exp(-s) ds \\ &= P(L, \beta x) \end{aligned}$$

where $P(a, x)$ is the incomplete gamma function (see [2]).

The theoretical expressions for mean and variance of such *pdf* as shown in the equation (4) are as follows:

$$E[x] = \frac{L}{\beta}$$

and

$$Var[x] = \frac{L}{\beta^2}$$

where E is the expectation and Var the variance operator. The moment estimators here are given by:

$$\hat{L} = \frac{\hat{m}_1^2}{\hat{m}_2 - \hat{m}_1^2}$$

and

$$\hat{\beta} = \frac{\hat{m}_1}{\hat{m}_2 - \hat{m}_1^2}$$

where $\hat{m}_r = \frac{1}{M}\sum_{i=0}^{M-1} x_i^r$, $r = 1, 2$ for any given data $\{x_i\}_{i=0}^{M-1}$.

4.3 Ship Detection Algorithm

An automatical ship detection model, which is a modification made on the initial algorithm in [5], is presented in [1]. In short, that ship detector model is divided into two parts. The first part is used to identify almost all visible ship targets in a SAR image. In actual, it uses a threshold which corresponds to a significance level to identify possible pixels and, after that, a morphological filter is applied to eliminate those false ship pixels. The second part is mainly to refine some ship targets by using simple thresholding and Radon transform techniques.

Unfortunately, the detection is limited in those images with 8 bits and no land regions occured in them. Presently, our strategy is to detect all possible ship targets in RADARSAT SAR images (with 16 bits) from coastal regions. For this purpose, we need to improve the detection model discussed in [1]. A new ship detection algorithm is described by the following steps:

Step 1: *Input SAR image data*

Step 2: *Find a pdf with a goodness-of-fit for the histogram of SAR image*

- *First estimating those parameters in K-distribution, if they are not large enough, then we use the K-model; otherwise*
- *Gamma-distribution will be considered as the pdf*

Step 3: *Determining a threshold I_c by the CFAR:*

- *Computation of $F(x) = \int_0^x p(t)dt$*
- *The threshold I_c should satisfy*

$$F(I_c) \leq \eta_c < F(I_c + 1)$$

Step 4: *Thresholding to identify possible ship pixels*

Step 5: *Reducing the false alarm rate (FAR) by the cleaning operation*

Step 6: *Output of the ship detection result*

5 Experimental Results

As discussed above, the first process in our model is to distinguish sea from land in an image with the coastal region. A potential detection method is proposed in Section 3. Next step, we try to detect all possible ship targets in the sea region. The main problem here is to determine an analytical solution of I_c. After a simple thresholding by I_c, a morphological filter is applied to eliminate those false ship pixels The filter is a 7 by 7 moving window. Each image pixel in the sea region is examined by placing it in the filter centre. The filter then examines the 48 neighbouring pixels. If more than 7 neighbouring pixels are possible ship pixels, the centre pixel is considered as a true ship pixel.

The model developed is tested on a number of SAR images with 16 bits. Three examples are shown in the following. The figures and tables present the detection results based on our model.

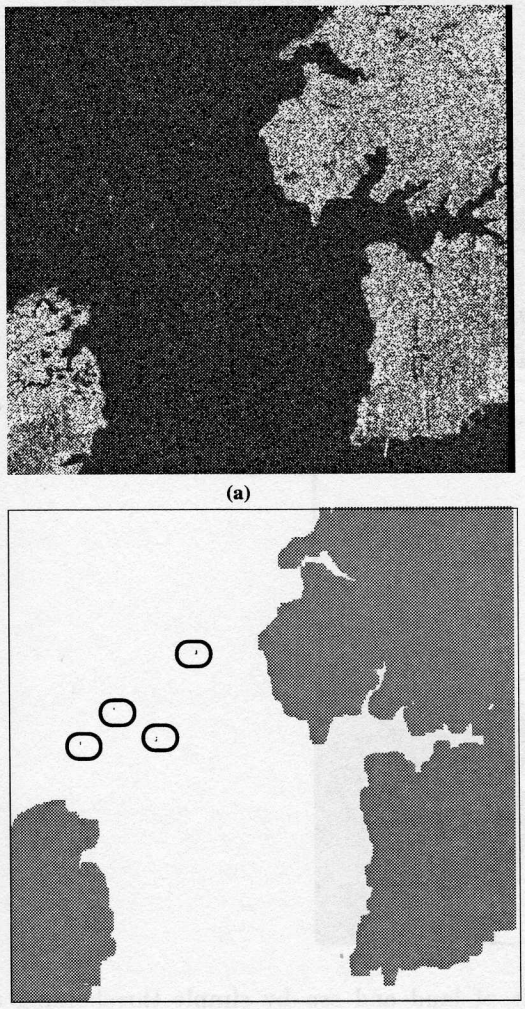

(a)

(b)

Figure 4: (a) Original image (1000 × 1000 pixels), (b) final detection result

Threshold T	32767
Threshold I_c	38080
CPU time (seconds)	89.01

Table 1: Thresholds and computational time corresponding to Fig. 4

6 Conclusions

We have demonstrated one possible method of automatic ship detection in RADARSAT SAR imagery. The program for this detection model has been developing in the C programming language and UNIX operational system. Further development is on the way to improve the applicability of our model and to reduce the computational time and false alarms.

Acknowledgment: We thank Dr. Maria T. Rey (DREO) for providing RADARSAT SAR images.

References

[1] Jiang, Q, S. Wang, D. Ziou, G. B. Bni, A. El Zaart, M. Rey, and M. Hensche, "Ship Detection in RADARSAT SAR Imagery", *Proceedings of IEEE SMC'98* (San Diego) pp4562-4566.

[2] Press W. H., W. T. Vetterling, S. A. Teukolsky, and B. P. Flanney, *Numerical Recipes in C*, Cambridge Univ. Press, 1992.

[3] M. Rey, J. K. E. Tunaley, J. T. Folinsbee, P. A. Jahans, J. A. Dixon, and M. R. Vant, "Application of radon transform techniques to wake detection of Seasat-A SAR images", *IEEE Transactions on Geoscience and Remote Sensing* Vol. 28, No. 4 (1990) 553-560.

[4] Rey M. T., T. Drosopoulos, and D. Petrovic, "A search procedure for ships in RADARSAT imagery" *DREO Report No. 1305*, 1996.

[5] Vachon P. W., J. Campbell, C. Bjerklund, F. Dobson, and M. Rey, "Ship detection by the RADARSAT SAR: Validation of detection model predictions", *Canadian Journal of Remote Sensing*, Vol. 23, No. 1 (1997) pp48-59.

[6] Lin I-I, L. K. Kwoh, Y. C. Lin, and V. Khoo, "Ship and ship wake detection in the ERS SAR imagery using computer-based algorithm", *IGARSS'97*.

[7] K. Eldhuset, "An automatic ship and ship wake detection system for space-borne SAR images in coastal regions", *IEEE Transactions on Geoscience and Remote Sensing* Vol. 34, No. 4 (1996) 1010-1019.

[8] K. Eldhuset, "Automatic ship and ship wake detection in space-borne SAR images from coastal regions", *Proceedings of IGARSS'88 Symposium,* ESA SP-284 (1988) 1529-1533.

[9] Norwegian Defence Research Establishment, *SAR Detection of ships and ship wakes*, European Space Agency Contract Report, 1988.

[10] Michael D. Henschel, R. B. Olsen, P. Hoyt, and Paris W. Vachon, "The Ocean Monitoring Workstation: Experience Gained with RADARSAT", 1998.

[11] Jiang, Q, E. Aitnouri, S. Wang, and D. Ziou, "Ship Detection in RADARSAT SAR Imagery using PNN-model", *Proceedings of ADRO Symposium'98* (Montreal).

[12] Jiang, Q., "Statistical Modelling for RADARSAT SAR Imagery and its Applications in Ship Target Detection", *PhD Thesis, University of Sherbrooke* (in preparation).

[13] Ali El Zaart, D. Ziou, S. Wang, and Q. Jiang, "Optimal Thresholding of RADARSAT SAR Images for Oil Slick Detection", *Proceedings of ADRO Symposium'98* (Montreal), 1998.

[14] Yanasse C. C. F., A. C. Frery, *et al.*, "Statistical Analysis of SAREX data over TAPAJS-Brazil", *Final Results Workshop for SAREX-92*, Paris, 1993.

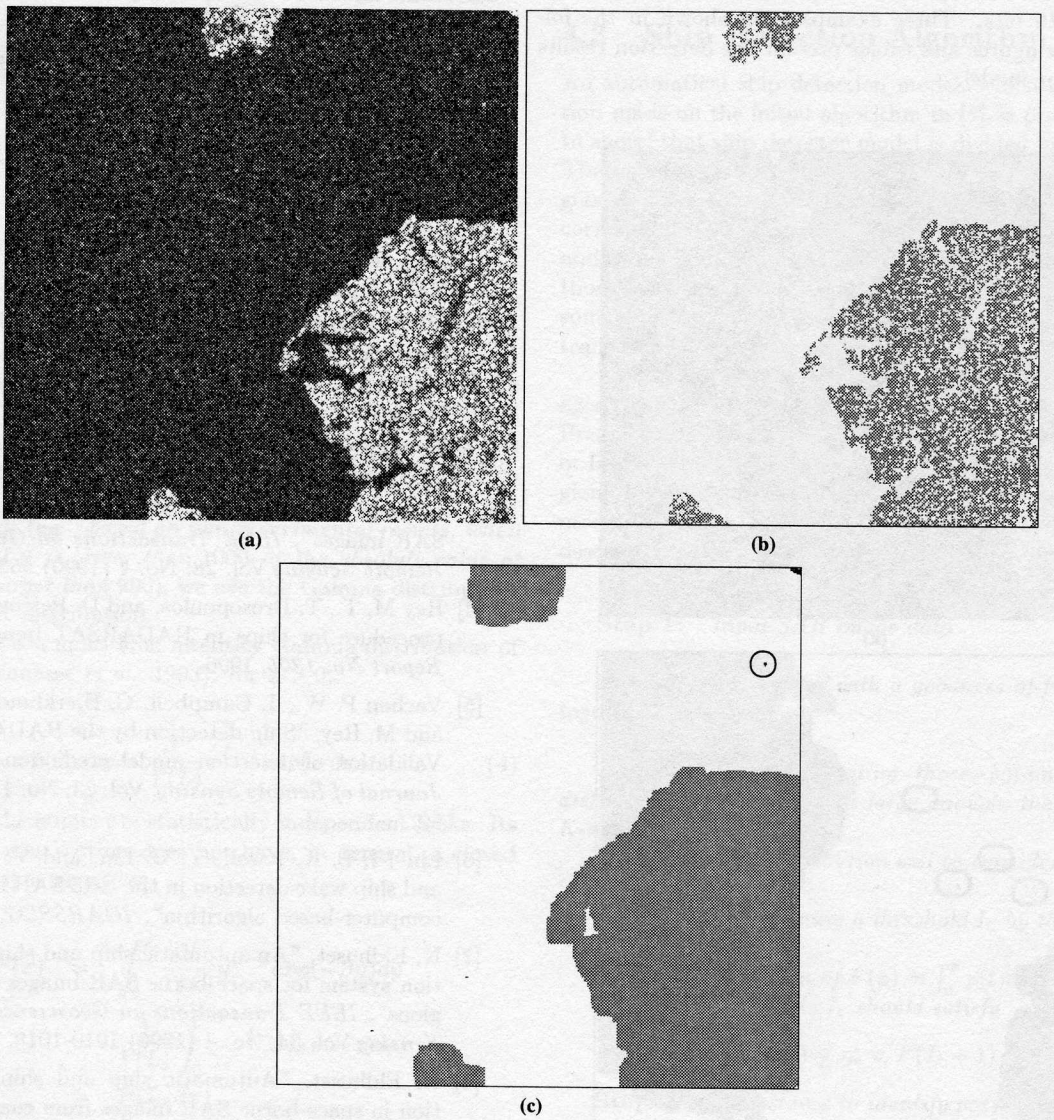

Figure 5: (a) Original image (512 × 512 pixels), (b) result of land and sea by simple thresholding and cleaning, (c) final detection result

Threshold T	32769
Threshold I_c	37205
CPU time (seconds)	16.25

Table 2: Thresholds and computational time corresponding to Fig. 5

Threshold T	32776
Threshold I_c	32892
CPU time (seconds)	6.63

Table 3: Thresholds and computational time corresponding to Fig. 6

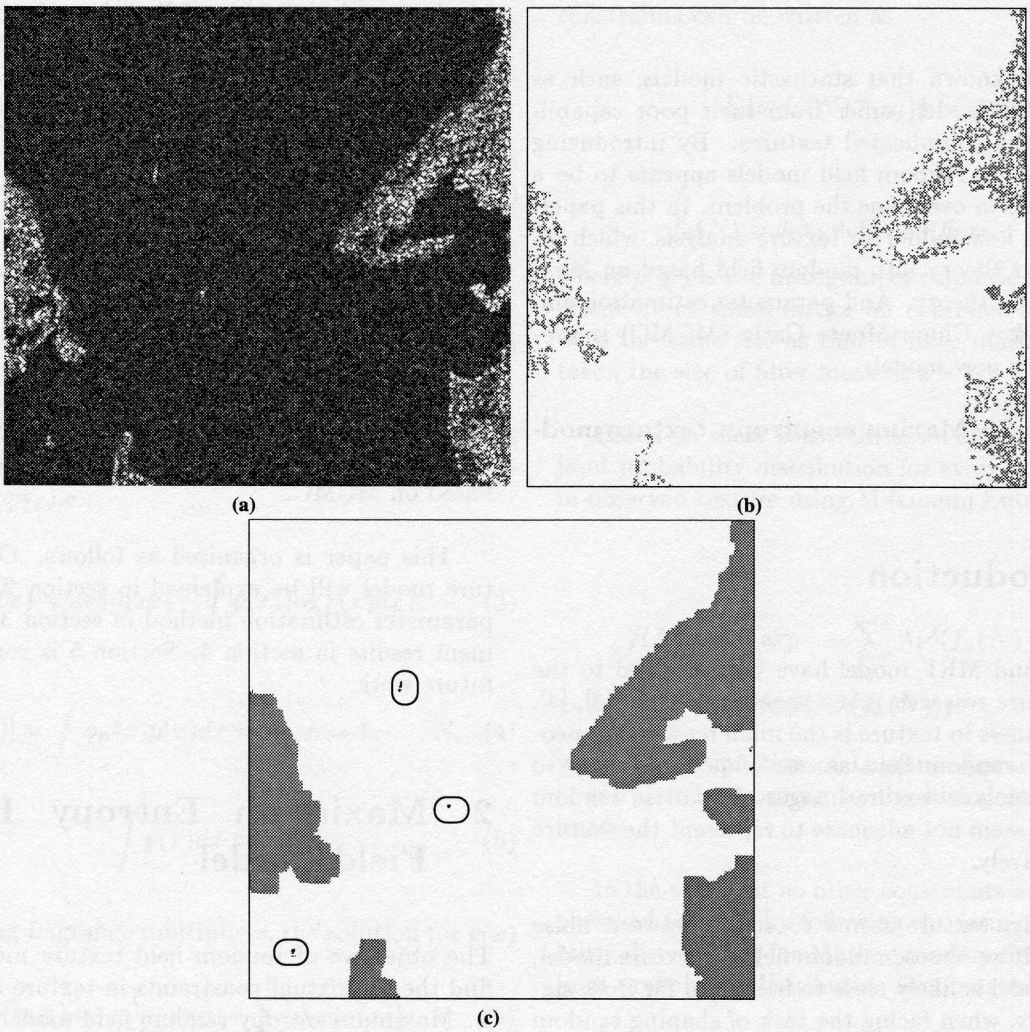

Figure 6: (a) Original image (512×512 pixels), (b) result of land and sea by simple thresholding and cleaning, (c) final detection result